

A Machine Learning Approach to Contact Localization in Variable Density Three-Dimensional Tactile Artificial Skin

Carson Kohlbrenner[†] Mitchell Murray[†] Yutong Zhang[†] Caleb Escobedo

Thomas Dunnington Nolan Stevenson Nikolaus Correll Alessandro Roncone

Department of Computer Science, University of Colorado Boulder

[†] represents equal contributions.

name . surname@colorado . edu

Abstract

Estimating the location of contact is a primary function of artificial tactile sensing apparatuses that perceive the environment through touch. Existing contact localization methods use flat geometry and uniform sensor distributions as a simplifying assumption, limiting their ability to be used on 3D surfaces with variable density sensing arrays. This paper studies contact localization on an artificial skin embedded with mutual capacitance tactile sensors, arranged non-uniformly in an unknown distribution along a semi-conical 3D geometry. A fully connected neural network is trained to localize the touching points on the embedded tactile sensors. The studied online model achieves a localization error of 5.7 ± 3.0 mm. This research contributes a versatile tool and robust solution for contact localization that is ambiguous in shape and internal sensor distribution.

1 Introduction

Artificial skin sensors are a direct way to measure external contact and have a wide range of applications in healthcare [2, 11], prosthetics, and robotics [25, 4]. As robots are increasingly deployed in close proximity to humans, the ability to localize where touch occurs allows actuating bodies to react appropriately to detected contact, interactable objects, and obstacles.

Artificial skin that is capable of localizing contact to a greater number of points on its sensor array than the number of sensors present is currently limited to flat surfaces [6, 11, 24, 26]. The localization methods used are typically constrained by assuming either a flat plate array or a uniform density of sensors. This paper presents a method of localizing contact on 3D artificial skin with non-uniform sensor distribution.

We present a curved, variable-density artificial skin equipped with mutual capacitance sensors that detect touch on the surface of the artificial skin. A neural network infers a relationship between the sensor readings and the geometry of the tactile skin. We evaluate this model by comparing known

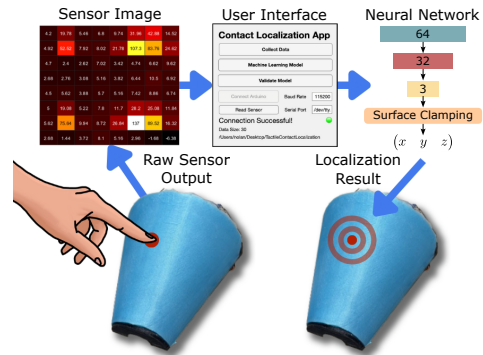


Figure 1: Contact localization model takes in a sensor image from any configuration of artificial tactile skin and determines the location of touch through a feedforward neural network.

touch locations to those returned by the model to characterize the accuracy and uncertainty. Our model robustly localizes the touching region on the 3D skin with variable sensor distribution. The code is available at <https://github.com/HIRO-group/TactileContactLocalization>

2 Related Work

Artificial skin sensors have a range of sensing methods such as acoustics [23, 21], computer vision [3, 8–10, 1], capacitive sensing [22, 7, 12–14, 18, 24, 16], electrical resistance tomography (ERT) [20, 19], and fiber Bragg grating (FBG) optical sensing [17]. Artificial skins composed of sensor arrays have increased scalability and conformity to non-flat geometries compared to computer vision tactile sensors. Our artificial skin uses a low-cost mutual capacitance sensing array method that is highly flexible to shape and size during fabrication.

Explicit contact localization methods can achieve high accuracies with capacitive sensor arrays and are standard in touchscreens and artificial skins with known sensor distributions [22, 19]. These explicit methods utilize the known positions of sensors to interpret locations of contact. Machine learning has been used in previous artificial skins to enhance contact localization accuracy with known sensor locations due to its ability to learn complex patterns [17, 15]. Our method treats capacitive sensor readings as images and uses a neural network to bypass the embedded spatial distribution of sensors by directly learning touch localization patterns.

3 Method

3.1 Fabrication

A challenge in implementing an artificial sensing skin array on a 3D object is conforming the sensing array to a curved surface. This is addressed by fabricating a two-dimensional sheet embedded with sensors, and then overlaying the artificial skin onto a semi-conical surface.

As shown in Fig. 2, the curved surface is outfitted with a total of 16 wires, divided evenly into 8 transmit and 8 receive elements, forming a network of 64 intersections. These intersections serve as the loci for capacitance measurements, effectively creating 64 sensors distributed across the surface. A mutual capacitance board (Muca) attached to the wires measures the capacitance values at each intersection [22]. A layer of 6mm thick silicone rubber is then molded on top of the wiring to provide a dielectric layer between wire intersections to ensure effective capacitive sensing. A thin copper sheet affixed to the underside of the 3D-printed structure functions as the grounding plate, mitigating electromagnetic noise from beneath the artificial skin. The result is a flush, $14.2 \times 16.4 \times 8.1$ cm semi-conical surface capable of contact localization through mutual capacitive sensing.

3.2 Calibration

The calibration process includes collecting a small dataset in a given operational environment to establish a correlation between raw capacitance readings and specific touch locations in 3D space. Each pair of raw sensor readings corresponding to a touch location are referred to as a "point log". Data is gathered by touching the artificial skin with an index finger at known locations. Two methodologies are employed for collecting point logs: random sampling and even spacing. For random sampling, the location is chosen as a point on a randomly selected edge from the CAD model of the skin. For even spacing, the surface of the CAD model is discretized into evenly spaced points depending on the selected number of point logs. When the skin sensor array is touched, 50 samples of the capacitance readings for each sensor are stored and correlated to the prompted touch position. This process is repeated until the desired number of point logs has been processed.

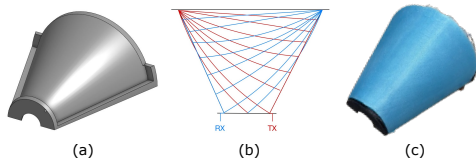


Figure 2: (a) CAD model for the curved geometry. (b) General wiring scheme. Sensors are located at each intersection of transmitter (TX) and receiver (RX) wires. (c) Fabricated skin sensor array where the sensing circuits are embedded within a layer of silicone.

the surface. A mutual capacitance board (Muca) attached to the wires measures the capacitance values at each intersection [22]. A layer of 6mm thick silicone rubber is then molded on top of the wiring to provide a dielectric layer between wire intersections to ensure effective capacitive sensing. A thin copper sheet affixed to the underside of the 3D-printed structure functions as the grounding plate, mitigating electromagnetic noise from beneath the artificial skin. The result is a flush, $14.2 \times 16.4 \times 8.1$ cm semi-conical surface capable of contact localization through mutual capacitive sensing.

3.3 Sensing

Mutual capacitance coupling occurs at the intersection of transmitter and receiver nodes. The intensity of the coupled capacitance can be measured by sending a known signal to the transmitter wire and measuring the signal of the receiver wire. The coupled capacitance is affected by grounded conductive objects entering the electromagnetic field near the intersection, such as a human finger. Grounded conductive objects reduce the measured capacitance at the receiver electrodes which correlates to higher contact outputs for a particular sensor.

The accuracy of the sensor measurements is determined by their noise levels through a signal-to-noise ratio. Fifty sensor measurements are taken for every point log and calibration measurement. Using these measurement samples, the average sensor values for each point log (\bar{S}), the average initial sensor values without contact (S_0), and the standard deviation from the average sensor value without contact (σ_0) are used to calculate the signal-to-noise ratio (SNR) of each sensor, i , within the sensor array using Eq. 1.

$$SNR_i = 20 \log_{10} \left(\frac{\max(\bar{S}_i) - S_{i,0}}{\sigma_{i,0}} \right) \quad (1)$$

3.4 Contact Localization Model

We use a supervised fully-connected neural network to localize the touching point based on raw sensor readings. This type of model is a low computation method of translation from raw sensor inputs to spatial predictions due to the nature of the artificial skin sensor data, as explained in Section 3.3. In the ideal scenario with zero sensor noise, a sensor image exists for every possible touch position along the surface of the skin. A sensor image is the full set of sensor values for a single touch and shown in Fig 1. Although this sensor image is also dependent on the probing finger and background electromagnetic field capacitance, we will assume these variables remain constant for this experiment by testing with the same finger and without changing locations for the duration of collecting data. A newly recorded sensor image can therefore be linked to a unique location along the surface of the skin once the relationship between the sensor image and position is established through our trained model.

The advantage of this method as opposed to algorithmic statistical estimation approaches is that it does not require the locations of the sensors within the skin to be known. The neural network uses a mean square error loss to compare the predicted touch locations from the sensor images collected during the calibration process against the associated given probe locations. A single hidden layer with 32 hidden nodes is trained to minimize the loss using gradient descent. To constrain the output to the surface of the skin, the predicted output from the model is compared to a set of discrete points on the surface of the skin. The point on the surface with the shortest distance to the predicted location of the model is used as the final prediction. This process effectively constrains the model to strictly output points on the surface of the skin.

4 Results

Multiple sets of training data are collected with a varied number of point logs to analyze the accuracy of the contact localization model. Fig. 4(b) shows the prediction error for a validation set of 20 random point logs tested for accuracy using contact localization models trained with 20, 50, 80, and 100 point logs, respectively. Data collection took approximately 1-2 minutes for every 20 point logs. The results show a trend of increasing the number of point logs used to train the model decreases the overall error in touch detection. However, on our skin array, this decrease in error levels off at about 80 point logs. Our best model has an accuracy of $5.7 \pm 3.0\text{mm}$.

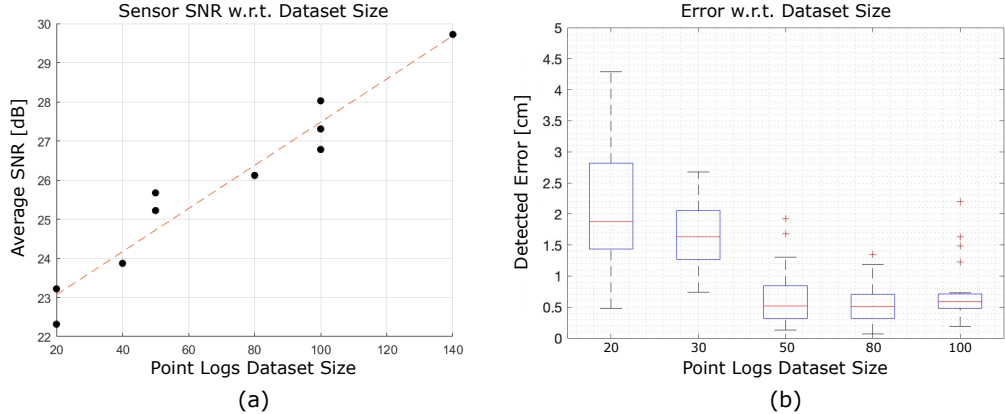


Figure 4: (a) The linear relationship between SNR and point logs dataset size suggests correlation. (b) Prediction error for contact localization models trained with varying sets of point logs.

The average SNR of all 64 sensors in the skin array is $< 30 \text{ dB}$. Fig. 4(a) shows the resulting SNR values for each trained model that we have tested. There exists a linear relationship between the quantity of point logs used in training the model and SNR values. The proportional increase in SNR with calibration dataset size may be due to a wider range of activation throughout the embedded sensors during calibration.

5 Discussion

This paper studies a machine learning approach to contact localization on an artificial skin embedded with mutual capacitance tactile sensors, arranged non-uniformly in a semi-conical geometry. This model only requires a CAD model and touch data to distinguish the relationships between a sensor image and touch location. We demonstrate this using a complex and unmeasured internal sensor distribution. This paper demonstrates that it is unnecessary to locate the placement of internal sensors in artificial skin to acquire accurate touch predictions. Changes in sensor location due to skin deformation that is incurred through conformation to various surface geometries may be navigated through neural network adaptability rather than altering the fabrication and calibration design. Our method achieved a better average localization accuracy than human skin and comparable results to artificial sensors with non-uniform sensor distribution methods.

One of the biggest limitations of our current implementation is the lack of precise visual cues during the data collection process, resulting in probing inaccuracies apart from the model inaccuracies. To improve this, we propose the application of a grid pattern to the surface of the skin with discrete touch locations. This grid can be loaded into the contact localization model and integrated into the data collection process reducing the error between the intended and actual touch locations. In addition, this research has only been conducted using single-touch interactions. Future work aims at identifying multi-touch accuracy and gesture identification, such as swiping up or down, which will drive its application toward robot-human communication through touch.

References

[1] Iris Andrussov, Huanbo Sun, Katherine J Kuchenbecker, and Georg Martius. Minsight: A fingertip-sized vision-based tactile sensor for robotic manipulation. *Advanced Intelligent Systems*, page 2300042, 2023.

Sensor Type	Known Locations	Acuity (mm)
Human Calf [5]	No	≈ 50.0
ERT [19]	Yes	6.6 ± 3.3
Curved Cap. (Ours)	No	5.7 ± 3.0
Human Fingertip [5]	No	≈ 4.0
FBG [17]	Yes	3.2 ± 2.3
Flat Cap. [22]	Yes	0.5 ± 0.2

Figure 5: Our mutual capacitance sensor achieves spatial acuity consistent with sensing arrays of known distributions and human skin.

- [2] Rachael Bevill Burns, Hasti Seifi, Hyosang Lee, and Katherine J Kuchenbecker. Getting in touch with children with autism: Specialist guidelines for a touch-perceiving robot. *Paladyn, Journal of Behavioral Robotics*, 12(1):115–135, 2020.
- [3] Wei Chen, Heba Khamis, Ingvars Birznieks, Nathan F Lepora, and Stephen J Redmond. Tactile sensors for friction estimation and incipient slip detection—toward dexterous robotic manipulation: A review. *IEEE Sensors Journal*, 18(22):9049–9064, 2018.
- [4] Gordon Cheng, Emmanuel Dean-Leon, Florian Bergner, Julio Rogelio Guadarrama Olvera, Quentin Leboutet, and Philipp Mittendorfer. A comprehensive realization of robot skin: Sensors, sensing, control, and applications. *Proceedings of the IEEE*, 107(10):2034–2051, 2019.
- [5] Giulia Corniani and Hannes P Saal. Tactile innervation densities across the whole body. *Journal of Neurophysiology*, 124(4):1229–1240, 2020.
- [6] Abu Bakar Dawood, Claudio Coppola, and Kaspar Althoefer. Learning decoupled multi-touch force estimation, localization and stretch for soft capacitive e-skin. *arXiv preprint arXiv:2303.05936*, 2023.
- [7] Yitao Ding, Felix Wilhelm, Leonhard Faulhammer, and Ulrike Thomas. With proximity servoing towards safe human-robot-interaction. In *2019 IEEE/RSJ International Conference on Intelligent Robots and Systems (IROS)*, pages 4907–4912. IEEE, 2019.
- [8] Won Kyung Do and Monroe Kennedy. Densetact: Optical tactile sensor for dense shape reconstruction. In *2022 International Conference on Robotics and Automation (ICRA)*, pages 6188–6194. IEEE, 2022.
- [9] Won Kyung Do, Bianca Jurewicz, and Monroe Kennedy. Densetact 2.0: Optical tactile sensor for shape and force reconstruction. In *2023 IEEE International Conference on Robotics and Automation (ICRA)*, pages 12549–12555. IEEE, 2023.
- [10] Siyuan Dong, Wenzhen Yuan, and Edward H Adelson. Improved gelsight tactile sensor for measuring geometry and slip. In *2017 IEEE/RSJ International Conference on Intelligent Robots and Systems (IROS)*, pages 137–144. IEEE, 2017.
- [11] Zackory Erickson, Henry M Clever, Vamsee Gangaram, Greg Turk, C Karen Liu, and Charles C Kemp. Multidimensional capacitive sensing for robot-assisted dressing and bathing. In *2019 IEEE 16th International Conference on Rehabilitation Robotics (ICORR)*, pages 224–231. IEEE, 2019.
- [12] Dirk Goeger, Matthias Blankertz, and Heinz Woern. A tactile proximity sensor. In *SENSORS, 2010 IEEE*, pages 589–594. IEEE, 2010.
- [13] Dirk Göger, Hosam Alagi, and Heinz Wörn. Tactile proximity sensors for robotic applications. In *2013 IEEE International Conference on Industrial Technology (ICIT)*, pages 978–983. IEEE, 2013.
- [14] Takayuki Hoshi and Hiroyuki Shinoda. Robot skin based on touch-area-sensitive tactile element. In *Proceedings 2006 IEEE International Conference on Robotics and Automation, 2006. ICRA 2006.*, pages 3463–3468. IEEE, 2006.
- [15] Maged Iskandar, Alin Albu-Schäffer, and Alexander Dietrich. Intrinsic sense of touch for intuitive physical human-robot interaction. *Science Robotics*, 9(93):eadn4008, 2024.
- [16] Perla Maiolino, Marco Maggiali, Giorgio Cannata, Giorgio Metta, and Lorenzo Natale. A flexible and robust large scale capacitive tactile system for robots. *IEEE Sensors Journal*, 13(10):3910–3917, 2013.
- [17] Luca Massari, Giulia Fransvea, Jessica D’Abbraccio, Mariangela Filosa, Giuseppe Terruso, Andrea Aliperta, Giacomo D’Alesio, Martina Zaltieri, Emiliano Schena, Eduardo Palermo, et al. Functional mimicry of ruffini receptors with fibre bragg gratings and deep neural networks enables a bio-inspired large-area tactile-sensitive skin. *Nature Machine Intelligence*, 4(5):425–435, 2022.

- [18] Stefan Escaida Navarro, Maximiliano Marufo, Yitao Ding, Stephan Puls, Dirk Göger, Björn Hein, and Heinz Wörn. Methods for safe human-robot-interaction using capacitive tactile proximity sensors. In *2013 IEEE/RSJ International Conference on Intelligent Robots and Systems*, pages 1149–1154. IEEE, 2013.
- [19] Kyungseo Park and Jung Kim. Neural-gas network-based optimal design method for ert-based whole-body robotic skin. *IEEE Transactions on Robotics*, 38(6):3463–3478, 2022.
- [20] Kyungseo Park, Hyunkyu Park, Hyosang Lee, Sungbin Park, and Jung Kim. An ert-based robotic skin with sparsely distributed electrodes: Structure, fabrication, and dnn-based signal processing. In *2020 IEEE International Conference on Robotics and Automation (ICRA)*, pages 1617–1624. IEEE, 2020.
- [21] Siddharth Rupavatharam, Caleb Escobedo, Daewon Lee, Colin Prepscious, Larry Jackel, Richard Howard, and Volkan Isler. Sonicfinger: Pre-touch and contact detection tactile sensor for reactive pregrasping. In *2023 IEEE International Conference on Robotics and Automation (ICRA)*, pages 12556–12562. IEEE, 2023.
- [22] Marc Teyssier, Brice Parilusyan, Anne Roudaut, and Jürgen Steimle. Human-like artificial skin sensor for physical human-robot interaction. In *2021 IEEE International Conference on Robotics and Automation (ICRA)*, pages 3626–3633. IEEE, 2021.
- [23] Vincent Wall, Gabriel Zöller, and Oliver Brock. Passive and active acoustic sensing for soft pneumatic actuators. *The International Journal of Robotics Research*, 42(3):108–122, 2023.
- [24] Yung-Chen Wang, Tsun-Yi Chen, Rongshun Chen, and Cheng-Yao Lo. Mutual capacitive flexible tactile sensor for 3-d image control. *Journal of microelectromechanical systems*, 22(3):804–814, 2013.
- [25] Jun Chang Yang, Jaewan Mun, Se Young Kwon, Seongjun Park, Zhenan Bao, and Steve Park. Electronic skin: recent progress and future prospects for skin-attachable devices for health monitoring, robotics, and prosthetics. *Advanced Materials*, 31(48):1904765, 2019.
- [26] Zhenxuan Zhao, Jianshi Tang, Jian Yuan, Yijun Li, Yuan Dai, Jian Yao, Qingtian Zhang, Sanchuan Ding, Tingyu Li, Ruirui Zhang, et al. Large-scale integrated flexible tactile sensor array for sensitive smart robotic touch. *ACS nano*, 16(10):16784–16795, 2022.